

## Enhancement of quasiparticle recombination in Ta and Al superconductors by implantation of magnetic and nonmagnetic atoms

R. Barends,<sup>1</sup> S. van Vliet,<sup>1</sup> J. J. A. Baselmans,<sup>2</sup> S. J. C. Yates,<sup>2</sup> J. R. Gao,<sup>1,2</sup> and T. M. Klapwijk<sup>1</sup>  
<sup>1</sup>*Kavli Institute of NanoScience, Faculty of Applied Sciences, Delft University of Technology,  
 Lorentzweg 1, 2628 CJ Delft, The Netherlands*

<sup>2</sup>*SRON Netherlands Institute for Space Research, Sorbonnelaan 2, 3584 CA Utrecht, The Netherlands*

(Received 22 December 2008; published 29 January 2009)

The quasiparticle recombination time in superconducting films, consisting of the standard electron-phonon interaction and a yet to be identified low-temperature process, is studied for different densities of magnetic and nonmagnetic atoms. For both Ta and Al, implanted with Mn, Ta, and Al, we observe an increase in the recombination rate. We conclude that the enhancement of recombination is not due to the magnetic moment, but arises from an enhancement of disorder.

DOI: [10.1103/PhysRevB.79.020509](https://doi.org/10.1103/PhysRevB.79.020509)

PACS number(s): 74.78.Db, 74.25.Nf, 74.40.+k

When a superconductor is perturbed, the equilibrium state is recovered by the recombination of excess quasiparticle excitations. Recombination is a binary reaction; quasiparticles with opposite wave vector and spin combine and join the superconducting condensate formed by the Cooper pairs, pairs of time-reversed electron states. The energy is transferred to the lattice by the material-dependent electron-phonon interaction<sup>1</sup> (symbolically represented in the lower inset of Fig. 1). With decreasing bath temperature the number of thermal quasiparticle excitations available for recombination reduces, and consequently the recombination time increases exponentially. There is, however, a discrepancy between this theory and experiments performed at low temperatures.<sup>2</sup> We have found that the relaxation saturates at low temperatures in both Ta and Al, indicating the presence of a second physical process which dominates low-temperature relaxation. The energy flux in hot-electron experiments suggests the same pattern.<sup>3</sup>

In the normal state it has become clear that a dilute concentration of magnetic atoms significantly enhances the inelastic scattering among quasiparticles.<sup>4,5</sup> In a superconductor the magnetic moment of the impurity leads to time-reversal symmetry breaking by spin-flip scattering, altering the superconducting state. The critical temperature  $T_c$  and energy gap  $\Delta$  decrease with increasing impurity concentration.<sup>6</sup> Depending on the magnetic atom and the host, localized impurity bound states as well as a band of states within the energy gap can appear.<sup>7-9</sup> In order to test the influence of magnetic impurities on the inelastic interaction in superconducting films, we have implanted both magnetic and nonmagnetic atoms and measured the relaxation times at temperatures far below the critical temperature.

We use the complex conductivity  $\sigma_1 - i\sigma_2$  to probe the superconducting state. The real part,  $\sigma_1$ , reflects the conduction by quasiparticles while the imaginary part,  $\sigma_2$ , arises from the accelerative response of the Cooper pairs, controlling the high-frequency ( $\omega$ ) response of the superconductor.<sup>10</sup> The restoration of the equilibrium state is measured by sensing the complex conductivity while applying an optical photon pulse. To this end, the superconducting film is patterned into planar quarter- and half-wavelength resonators, comprised of a meandering coplanar waveguide

(CPW) with a central line, 3  $\mu\text{m}$  wide, and metal slits, 2  $\mu\text{m}$  wide; see upper inset of Fig. 1 (for details see Refs. 2 and 11). The condensate gives rise to a kinetic inductance  $L_k \sim 1/d\omega\sigma_2$ , with  $d$  as the thin-film thickness, which controls the resonance frequency:  $\omega_0 = 2\pi/4l\sqrt{(L_g + L_k)C}$  for a quarter-wave resonator, with  $l$  the length,  $L_g$  the geometric inductance, and  $C$  as capacitance per unit length. Lengths of several millimeters are used, corresponding to resonance frequencies of typically 3–6 GHz. The resonators are capacitively coupled to a feedline. Upon optical excitation the complex conductivity reflects the change in the quasiparticle density  $n_{qp}$  by  $\delta\sigma_2/\sigma_2 = -\frac{1}{2}\delta n_{qp}/n_{Cp}$ , with  $n_{Cp}$  as the Cooper

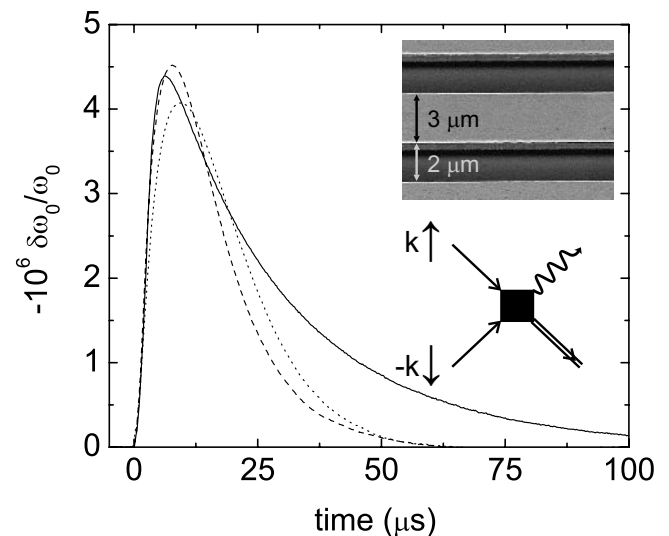


FIG. 1. The evolutions of the resonance frequency in response to an optical pulse (2  $\mu\text{s}$  duration) for a Ta sample (solid line), Ta implanted with 100 ppm Mn (dashed line), and 100 ppm Ta (dotted line) (average of 100 traces). The initial rise is due to the response time of the resonator. The subsequent exponential decay (Ta:  $\tau = 28 \mu\text{s}$ ; Ta with Mn:  $\tau = 11 \mu\text{s}$ ; Ta with Ta:  $\tau = 11 \mu\text{s}$ ) reflects the recovery of the equilibrium state [Eq. (1)]. The relaxation is due to recombination of quasiparticles into Cooper pairs (depicted in the lower inset). A scanning electron micrograph of the coplanar waveguide geometry of the resonator is shown in the upper inset. The width of the central line is 3  $\mu\text{m}$  and the width of the slits is 2  $\mu\text{m}$ .

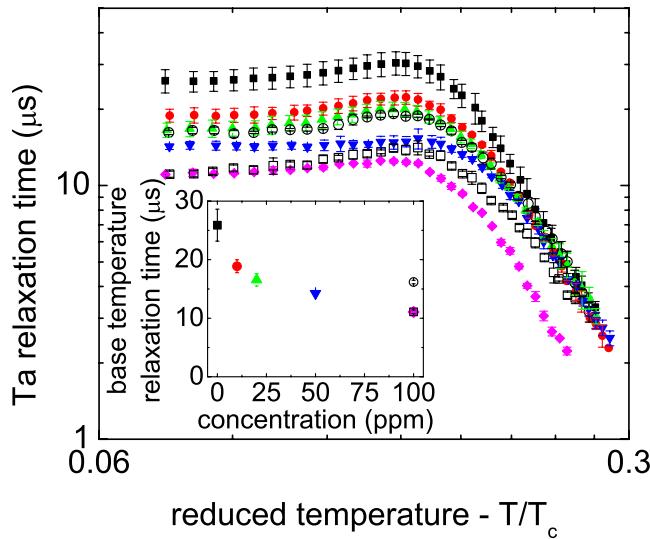


FIG. 2. (Color online) The relaxation time as a function of reduced bath temperature in Ta ( $T_c=4.4$  K) with ion-implanted concentrations of Mn: 0 (■), 10 (●), 20 (▲), 50 (▼), and 100 ppm (◆), as well as with 100 ppm Ta (□) and 100 ppm Al (○). The relaxation times at base temperature (325 mK) are plotted in the inset versus ion concentration.

pair density ( $n_{qp} \ll n_{Cp}$ ). The resonance frequency directly senses the variation in the superconducting state,

$$\frac{\delta\omega_0}{\omega_0} = \frac{\alpha}{2} \frac{\delta\sigma_2}{\sigma_2} (f(E), \Delta), \quad (1)$$

with  $f(E)$  as the distribution of quasiparticles over the energy and  $\alpha$  as the fraction of the kinetic to total inductance.

The resonators are made from Ta and Al. The Ta film, 280 nm thick, is sputter deposited onto a hydrogen-passivated, high-resistivity ( $>10$  k $\Omega$  cm), (100)-oriented Si substrate. A 6 nm Nb seed layer is used underneath the Ta layer to promote growth of the desired body-centered-cubic phase.<sup>12</sup> The film critical temperature is 4.4 K, the low-temperature resistivity ( $\rho$ ) is 8.8  $\mu\Omega$  cm, and the residual resistance ratio (RRR) is 3.2. The Al film, with a thickness of 100 nm, is sputtered onto a similar Si substrate ( $T_c=1.2$  K,  $\rho=0.81$   $\mu\Omega$  cm, and RRR=4.5). Patterning is done using optical lithography, followed by reactive ion etching for Ta and wet etching for Al. After patterning, various concentrations of Mn (as magnetic atom) and Ta and Al have been ion implanted. The Ta film has been implanted with Mn, Ta, and Al at energies of 500, 500, and 250 keV, respectively. The Al film has been implanted with Mn and Al at 60 and 30 keV, to place the peak of the concentration near the middle of the film.<sup>13</sup> The Ta samples are placed on a He-3 sorption cooler in a He-4 cryostat, with the sample space surrounded by a superconducting magnetic shield. The Al samples are placed on an adiabatic demagnetization refrigerator; here a superconducting shield and a Cryoperm shield are used. The optical pulse is provided by a GaAsP (1.9 eV) light-emitting diode (LED), which is fiber-optically coupled to the sample box. The transmission of the feedline near the resonance fre-

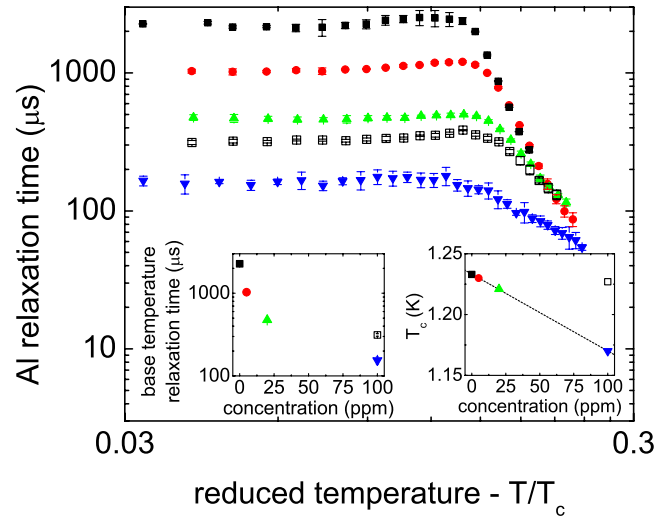


FIG. 3. (Color online) The relaxation time as a function of reduced bath temperature in Al with various ion-implanted concentrations of Mn: 0 (■), 5 (●), 20 (▲), and 100 ppm (▼), as well as with 100 ppm Al (□). The left inset shows the relaxation time at base temperature versus ion concentration. The critical temperature decreases only with increasing Mn concentration (right inset).

quency is sensed using a signal generator, a low-noise amplifier, and a quadrature mixer, allowing for monitoring the resonance frequency in the time domain.<sup>2,11</sup>

Typical optical pulse responses are shown in Fig. 1 for Ta quarter-wave resonators at the base temperature of 325 mK. The exponential decrease reflects the restoration of equilibrium in the superconducting state. The initial rise is due to the response time of the resonator. The faster decay indicates a faster relaxation for implanted Ta samples. The temperature dependence of the relaxation times is shown in Fig. 2 for Ta samples implanted with a range of concentrations from 0-100 ppm Mn, and with 100 ppm Ta and Al. At low temperatures a clear trend of a *decreasing* relaxation time with *increasing* impurity concentration is visible, both for samples implanted with Mn and samples implanted with Ta and Al. Below  $T/T_c \sim 0.1$  the relaxation times become independent of temperature, reaching plateau values of 26  $\mu$ s for the unimplanted samples, values down to 11  $\mu$ s for samples implanted with Mn, 11  $\mu$ s with Ta, and 16  $\mu$ s with Al, clearly decreasing with increasing impurity concentration (see inset of Fig. 2). Near  $T/T_c \sim 0.15$  the relaxation times reach a peak value in all samples. At high temperatures ( $T/T_c \geq 0.2$ ) we find that the relaxation times increase with decreasing temperature. Here, the relaxation times of the implanted samples, except for the sample with 100 ppm Mn, join with the values of the unimplanted sample, and is understood as due to the conventional electron-phonon process.<sup>2</sup> The critical temperature remains unchanged.

In Al samples, half-wave resonators, implanted with 0–100 ppm Mn or 100 ppm Al, the relaxation times follow a similar pattern; see Fig. 3. The effect of the implanted impurities is most significant at the lowest temperatures (below  $T/T_c \sim 0.1$ ), where the plateau value of the relaxation time is decreased by an order of magnitude: from a value of 2.3 ms for unimplanted Al down to 320  $\mu$ s for Al with 100 ppm Al

and 150  $\mu\text{s}$  for Al with 100 ppm Mn (see left inset). A slight nonmonotonic temperature dependence is observed for all samples. Above  $T/T_c \geq 0.2$  the relaxation times increase with decreasing temperature. In addition, the sample critical temperature decreases linearly with increasing Mn concentration (see right inset of Fig. 3), with  $\Delta T_c/\Delta c_{\text{Mn}} = -0.63$  mK/ppm (dashed line), while remaining unchanged when implanting Al.

We interpret the relaxation as due to the recombination of quasiparticles near the gap energy: first, we probe  $\sigma_2$  which is associated with the Cooper pairs. Second, identical relaxation times are found when creating quasiparticle excitations near the gap energy by applying a microwave pulse at the resonance frequency  $\omega_0$ . In addition, the data are not influenced by quasiparticle out-diffusion as no length dependence was observed in the Al half-wavelength resonators, where the central line is isolated from the ground plane and Ta quarter-wavelength resonators used. Moreover, the relaxation time is independent of the photon flux for the small intensities used. Furthermore, the samples are well isolated from thermal radiation: we observe no significant change in relaxation time when varying the temperature of the cryostat or of a blackbody placed next to the sample box. Finally, the significant effect of the implantation of impurities indicates that the relaxation time reflects the restoration of equilibrium in the superconducting films.

The data show a clear trend of decreasing relaxation time in both Ta and Al with an increasing ion-implanted impurity concentration. The significant decrease at the lowest temperatures indicates that the dominant low-temperature relaxation channel is enhanced, while the relaxation process at higher temperatures is less affected.

In a superconductor the magnetic nature of the atom depends on the coupling between its spin and the host conduction electrons. Mn has been shown to retain its magnetic moment in Nb, V,<sup>14</sup> and Pb,<sup>8</sup> acting as a pair breaker and giving rise to subgap states. On the other hand, when Mn is placed inside Al,  $s$ - $d$  mixing occurs: the localized  $d$  electron states of the transition-metal impurity strongly mix with the conduction band, resulting in the impurity effectively losing its magnetic moment as well as an increase in the Coulomb repulsion.<sup>15</sup> It acts predominantly as a pair weakener: suppressing superconductivity, yet contrary to the case of pair breaking, showing no evidence of subgap states.<sup>16</sup>

In order to quantify a possible influence of magnetic impurities on recombination we use the conventional theories by Zittartz, Bringer, and Müller-Hartmann<sup>17</sup> (ZBMH) and Kaiser.<sup>15</sup> In the presence of a pair-breaking impurity bound states develop within the energy gap near reduced energy  $\gamma$ . The quasiparticle excitations, denoted by the Green's function  $G$ , and the paired electrons  $F$  are described by  $E = u(\Delta + \Gamma \frac{\sqrt{1-u^2}}{u^2 - \gamma^2})$ , with  $G(E) = u(E)/\sqrt{u(E)^2 - 1}$ ,  $F(E) = i/\sqrt{u(E)^2 - 1}$ , and  $\Gamma = \hbar/\tau_{sf}$  as the pair-breaking parameter. For  $\gamma \rightarrow 1$  the Abrikosov-Gorkov (AG) and for  $\Gamma \rightarrow 0$  the BCS results are recovered, respectively. The normalized density of states is  $\text{Re}[G(E)]$ . The rate of recombination with phonon emission is<sup>1</sup>

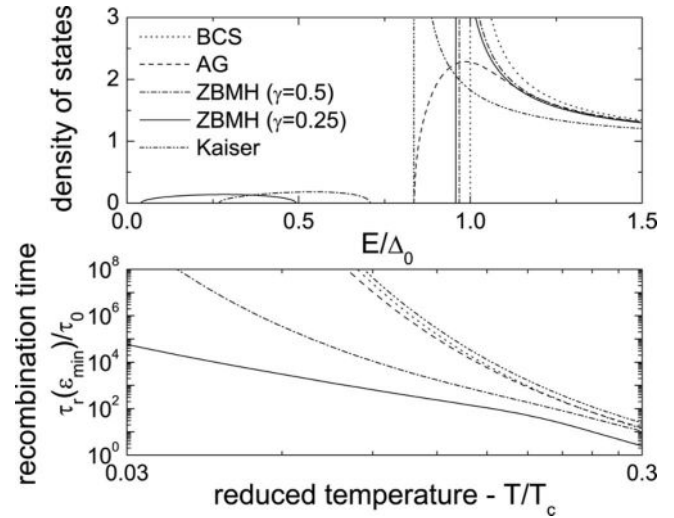


FIG. 4. Upper figure: Normalized quasiparticle density of states in the presence of magnetic impurities according to pair-breaking theories by AG as well as ZBMH ( $\Gamma/\Delta_0=0.03$ ) and the pair-weakening theory by Kaiser (Ref. 15) (for  $\Delta$  identical to that in the AG case). Lower figure: The corresponding recombination times, using Eq. (2).

$$\frac{1}{\tau_r(\epsilon)} = \frac{1}{\tau_0(kT_{c0})^3[1-f(\epsilon)]} \int_0^\infty (E+\epsilon)^2 \times \left( \text{Re}[G(E)] + \frac{\Delta}{\epsilon} \text{Im}[F(E)] \right) [n(E+\epsilon) + 1] f(E) dE, \quad (2)$$

with  $\tau_0$  denoting the material-dependent electron-phonon time, assuming for the electron-phonon spectral function that  $\alpha^2 F(E) \propto E^2$ , and with  $n(E)$  as the phonon distribution function. On the other hand, in the presence of pair weakening,  $T_c$  and  $\Delta$  are reduced simultaneously, and the exponential dependence of the recombination time on  $T/T_c$  is retained. In Fig. 4, the density of states (upper figure) and the recombination time for quasiparticles at the minimum excitation energy  $\epsilon_{\text{min}}$  (lower figure) are shown for different cases. Clearly, a density of states modified by magnetic impurities results in a recombination time which remains temperature dependent, independent of the model used. A particular model analysis was recently performed by Kozorezov *et al.*<sup>18</sup>

We conclude that the recombination processes are unrelated to the bulk magnetic moment of the implanted atoms, in agreement with the observation that an enhancement can also be established by implanting nonmagnetic atoms (Figs. 1–3). Instead we attribute the enhancement to an increase in the disorder caused by the implantation. Impurities might alter the electron-phonon interaction,<sup>19</sup>  $\tau_0$  in Eq. (2), but no saturation would result.<sup>2</sup>

An interesting role of disorder, in particular at the surface, has recently become apparent through phenomena controlled by unpaired magnetic surface spins. An enhancement of the critical current of nanowires has been observed,<sup>20</sup> in agreement with theoretical predictions in which surface spins are aligned by the magnetic field.<sup>21</sup> In addition, recent tunneling

measurements on niobium surfaces show subgap states (Fig. 4), signaling spins at the surface, possibly due to the native oxide.<sup>22</sup> Magnetic moments at surface defects were also proposed by Koch *et al.*<sup>23</sup> to explain the ubiquitous presence of flux noise in superconducting quantum interference devices (SQUIDs). Sendelbach *et al.*<sup>24</sup> observed in both Al and Nb SQUIDs a strong dependence of the flux on temperature, which they interpreted as due to paramagnetic ordering of surface spins by local fields in the vortex cores. In our recent experiments on the frequency noise of superconducting resonators, we also find a strong dependence on the surface properties.<sup>25</sup> In view of the other experiments, we conjecture that in our samples unpaired surface spins are present, whose density is enhanced by the ion bombardment. In order to properly address the relation to the recombination rate, Eq. (2) needs to be reanalyzed taking into account spin flip,<sup>26</sup> possible spin-glass formation,<sup>24</sup> and particle-hole asym-

metry,<sup>7</sup> giving rise to quasiparticles in the ground state.<sup>27</sup>

In conclusion, we have measured the relaxation time in Ta and Al superconducting films implanted with both magnetic and nonmagnetic impurities, using the complex conductivity. We find a clear trend of decreasing relaxation time with increasing implanted impurity concentration, independent of their magnetic moment. Our observations show that low-temperature quasiparticle recombination is enhanced by disorder, most likely involving the surface.

The authors thank Y. J. Y. Lankwarden for fabrication of the devices; K. van der Tak for the ion implantation; Ya. M. Blanter, T. T. Heikkilä, and Yu. V. Nazarov for stimulating discussions; and H. F. C. Hoevers for support. The work was supported by RadioNet (EU), the Netherlands Organisation for Scientific Research (NWO), and the NanoSciERA “Nanofridge” project (EU).

- 
- <sup>1</sup>S. B. Kaplan, C. C. Chi, D. N. Langenberg, J. J. Chang, S. Jafarey, and D. J. Scalapino, *Phys. Rev. B* **14**, 4854 (1976).
- <sup>2</sup>R. Barends, J. J. A. Baselmans, S. J. C. Yates, J. R. Gao, J. N. Hovenier, and T. M. Klapwijk, *Phys. Rev. Lett.* **100**, 257002 (2008).
- <sup>3</sup>A. V. Timofeev, C. Pascual García, N. B. Kopnin, A. M. Savin, M. Meschke, F. Giazotto, and J. P. Pekola, *Phys. Rev. Lett.* **102**, 017003 (2009).
- <sup>4</sup>A. Anthore, F. Pierre, H. Pothier, and D. Esteve, *Phys. Rev. Lett.* **90**, 076806 (2003).
- <sup>5</sup>B. Huard, A. Anthore, N. O. Birge, H. Pothier, and D. Esteve, *Phys. Rev. Lett.* **95**, 036802 (2005).
- <sup>6</sup>A. A. Abrikosov and L. P. Gorkov, *Sov. Phys. JETP* **12**, 1243 (1961).
- <sup>7</sup>A. Yazdani, B. A. Jones, C. P. Lutz, M. F. Crommie, and D. M. Eigler, *Science* **275**, 1767 (1997).
- <sup>8</sup>W. Bauriedl, P. Ziemann, and W. Buckel, *Phys. Rev. Lett.* **47**, 1163 (1981).
- <sup>9</sup>L. Dumoulin, E. Guyon, and P. Nedellec, *Phys. Rev. B* **16**, 1086 (1977).
- <sup>10</sup>D. C. Mattis and J. Bardeen, *Phys. Rev.* **111**, 412 (1958).
- <sup>11</sup>P. K. Day, H. G. LeDuc, B. A. Mazin, A. Vayonakis, and J. Zmuidzinas, *Nature (London)* **425**, 817 (2003).
- <sup>12</sup>D. W. Face and D. E. Prober, *J. Vac. Sci. Technol. A* **5**, 3408 (1987).
- <sup>13</sup>J. F. Ziegler *et al.*, computer code SRIM-2008.01, 2008 ([www.srim.org](http://www.srim.org)).
- <sup>14</sup>A. Roy, D. S. Buchanan, D. J. Holmgren, and D. M. Ginsberg, *Phys. Rev. B* **31**, 3003 (1985).
- <sup>15</sup>A. B. Kaiser, *J. Phys. C* **3**, 410 (1970).
- <sup>16</sup>G. O’Neil, D. Schmidt, N. A. Miller, J. N. Ullom, A. Williams, G. B. Arnold, and S. T. Ruggiero, *Phys. Rev. Lett.* **100**, 056804 (2008).
- <sup>17</sup>J. Zittartz, A. Bringer, and E. Müller-Hartmann, *Solid State Commun.* **10**, 513 (1972).
- <sup>18</sup>A. G. Kozorezov, A. A. Golubov, J. K. Wigmore, D. Martin, P. Verhoeve, R. A. Hijmering, and I. Jerjen, *Phys. Rev. B* **78**, 174501 (2008).
- <sup>19</sup>J. Rammer and A. Schmid, *Phys. Rev. B* **34**, 1352 (1986).
- <sup>20</sup>A. Rogachev, T. C. Wei, D. Pekker, A. T. Bollinger, P. M. Goldbart, and A. Bezryadin, *Phys. Rev. Lett.* **97**, 137001 (2006).
- <sup>21</sup>M. Yu. Kharitonov and M. V. Feigel’man, *JETP Lett.* **82**, 421 (2005).
- <sup>22</sup>T. Proslir, J. F. Zasadzinski, L. Cooley, C. Antoine, J. Moore, J. Norem, M. Pellin, and K. E. Gray, *Appl. Phys. Lett.* **92**, 212505 (2008).
- <sup>23</sup>R. H. Koch, D. P. DiVincenzo, and J. Clarke, *Phys. Rev. Lett.* **98**, 267003 (2007).
- <sup>24</sup>S. Sendelbach, D. Hover, A. Kittel, M. Mück, John M. Martinis, and R. McDermott, *Phys. Rev. Lett.* **100**, 227006 (2008).
- <sup>25</sup>R. Barends, H. L. Hortensius, T. Zijlstra, J. J. A. Baselmans, S. J. C. Yates, J. R. Gao, and T. M. Klapwijk, *Appl. Phys. Lett.* **92**, 223502 (2008).
- <sup>26</sup>C. Grimaldi and P. Fulde, *Phys. Rev. Lett.* **77**, 2550 (1996).
- <sup>27</sup>M. E. Flatté and J. M. Byers, *Phys. Rev. B* **56**, 11213 (1997).